Class. Quantum Grav. **25** (2008) 184013 (10pp) doi:10.1088/0264-9381/25/18/184013

Search for continuous gravitational waves from PSR J0835-4510 using CLIO data

Tomomi Akutsu[1], Masaki Ando[2], Tomiyoshi Haruyama[3], Nobuyuki Kanda[4], Kazuaki Kuroda[1], Sinji Miyoki[1], Masatake Ohashi[1], Yoshio Saito[3], Nobuaki Sato[3], Takakazu Shintomi[5], Toshikazu Suzuki[3], Hideyuki Tagoshi[6], Hirotaka Takahashi[7], Daisuke Tatsumi[8], Souichi Telada[9], Takayuki Tomaru[3], Takashi Uchiyama[1], Akira Yamamoto[3] and Kazuhiro Yamamoto[10]

[1] Institute for Cosmic Ray Research, The University of Tokyo, Kashiwa, Chiba 277-8582, Japan
[2] Department of Physics, The University of Tokyo, Bunkyo-ku, Tokyo 113-0033, Japan
[3] High Energy Accelerator Research Organization, Tsukuba, Ibaraki 305-0801, Japan
[4] Department of Physics, Graduate School of Science, Osaka City University, Sumiyoshi-ku, Osaka, Osaka 558-8585, Japan
[5] Advanced Research Institute for the Sciences and Humanities, Nihon University, Chiyoda-ku, Tokyo 102-0073, Japan
[6] Department of Earth and Space Science, Graduate School of Science, Osaka University, Toyonaka, Osaka 560-0043, Japan
[7] Department of Management and Information Systems Science, Nagaoka University of Technology, Nagaoka, Niigata 940-2188, Japan
[8] National Astronomical Observatory of Japan, Mitaka, Tokyo 181-8588, Japan
[9] National Institute for Advanced Industrial Science and Technology, Tsukuba, Ibaraki 305-8563, Japan
[10] Albert-Einstein-Institut, Max-Planck-Institut für Gravitationsphysik, D-30167 Hannover, Germany

Received 18 April 2008, in final form 17 July 2008
Published 2 September 2008
Online at stacks.iop.org/CQG/25/184013

Abstract
We search for continuous gravitational waves from PSR J0835-4510 at twice its rotational frequency using CLIO (Cryogenic Laser Interferometric Observatory) in the Kamioka mine. In this search, we use data from an observational run during 12–28 February 2007. We give a brief description of the methods used in this search. We obtain an upper limit on gravitational wave amplitude for PSR J0835-4510 as $h_{0(\mathrm{UL})} = 5.3 \times 10^{-20}$ with 99.4% confidence level.

PACS numbers: 95.85.Sz, 04.80.Nn, 07.05Kf, 95.55Ym

1. Introduction

Several laser interferometric gravitational wave detectors have been designed and built to detect gravitational waves directly. They include LIGO [1], GEO [2], TAMA300 [3] and

VIRGO [4]. The direct detection of gravitational waves is important not only because it will become a new astronomical tool to observe our universe, but also because it will become a new tool to verify general relativity and other gravity theories in a strong gravity field.

A spinning neutron star is expected to emit gravitational waves if it is not perfectly symmetric about its rotational axis. Pulsars, spinning neutron stars, are one of the most important target sources for the gravitational wave detectors.

We select PSR J0835-4510 (Vela pulsar) as a target in this search. PSR J0835-4510 is known to be a relatively close pulsar, located at 250–500 pc [5]. The spin frequency and spin-down rate from radio observations give an upper limit on the gravitational wave amplitude, $h_0 \sim 4.9 \times 10^{-24}$, which is the largest among pulsars which correspond to the upper limit on the ellipticity of the neutron star, $\epsilon = 3.0 \times 10^{-3}$. The gravitational wave frequency of PSR J0835-4510 is about 22 Hz. To the best of our knowledge, this is the first analysis of a pulsar at a gravitational wave frequency below 50 Hz, since previous detectors did not have good sensitivity in frequency range below 50 Hz.

CLIO (Cryogenic Laser Interferometer Observatory) undertook a one week observation at room temperature from 12 to 18 February 2007. The CLIO had good sensitivity in the low-frequency range. In spite of short arm length (100 m), CLIO has demonstrated sensitivity at 20 Hz comparable to the km-scale detectors operating in the same period. The data from this observation provide a good opportunity to perform a search for gravitational waves produced by PSR J0835-4510.

In this paper, we present the results of the analysis of CLIO data to search for gravitational waves emitted from PSR J0835-4510. We use matched filtering for this search, which is an optimal method when a waveform is well predicted. The analysis method is based on [6]. Gravitational waves from pulsars are so faint that we need to integrate long term data in order to increase the signal-to-noise ratio (SNR). In order to reduce the computation time of the analysis, we compress the data with the complex heterodyne technique. In the matched filtering analysis, we need exact waveforms which depend on unknown parameters. In this analysis, there are two unknown parameters: the polarization angle and the inclination angle. These unknown parameters are searched for on the discrete grid point in a two-dimensional parameter space. The distance between grid points is determined so that there are at most a 2% loss of SNR. Searches are performed in a frequency range between -0.003 and 0.003 Hz around the target gravitational wave frequency.

This paper is organized as follows. In section 2, we give an overview of the detector and the data we analyze. In section 3 , we give an overview of the analysis methods. In section 4, the results of analysis are presented. In section 5, we summarize the results and present the conclusion.

2. Detector and data set

CLIO is a locked Fabry–Perot interferometer with a base line arm length of 100 m, located at the Kamioka mine (36.25° N, 137.18° E), 220 km west of Tokyo. The CLIO project also includes the apparatus for geophysics [7]. Basic information on the position, orientation of the detector and detailed descriptions of its operation can be found in [8]. One of the main purposes of CLIO is to demonstrate thermal–noise suppression by cooling the mirrors for a future Japanese project, LCGT (Large-scale Cryogenic Gravitational Telescope) [9]. The current best sensitivity at 300 K is about $6 \times 10^{-21}\sqrt{\text{Hz}}^{-1}$ around 400 Hz. Below 20 Hz, the strain sensitivity is comparable with that of LIGO, although the baselines of CLIO are 40 times shorter. This is because the seismic motion is extremely small in the Kamioka mine.

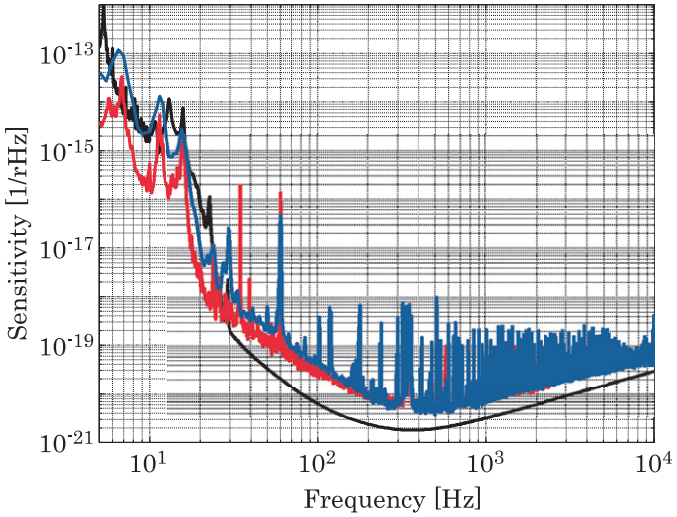

Figure 1. Sensitivity of the CLIO at the observation. The black line is the designed sensitivity at room temperature. The blue line is a sensitivity during the observation, and the red line is the best sensitivity of CLIO, respectively.

(This figure is in colour only in the electronic version)

The main signal of the detector, the feedback control signal and other auxiliary channel signals are recorded with a 65 536 Hz sampling frequency. We adopt a signal peak calibration method [10] in order to calibrate data from the detector. During the operation, the mirrors of the detector are actuated with a 512 Hz sinusoid for continuous calibration.

We have operated the interferometer at room temperature for the observation from 12 to 18 February 2007. Figure 1 shows a sensitivity during the observation. CLIO's observations were sometimes suspended when the interferometer lost the lock. They were also sometimes interrupted manually for maintenance. By removing such dead time, the total length of data available for this data analysis is 86 h.

3. Overview of the analysis methods

3.1. Signal model

In the matched filtering analysis, it is important to use very accurate templates. In the following, we present the signal model used in this search.

In order to make a precise signal waveform, we have to predict its phase evolution and the antenna pattern of the detector. Signal $h(t)$ of a pulsar which reaches the detector can be written as a linear combination of two polarizations multiplied by the corresponding sensitivity of the detector to that polarization:

$$h(t) = h_+(t)F_+(t) + h_\times(t)F_\times(t), \tag{1}$$

where $F_+(t)$ and $F_\times(t)$ are antenna-pattern functions which depend on time through the incident direction of gravitational wave. The two polarizations of waves, $h_+(t)$ and $h_\times(t)$, are written as follows [11]:

$$h_+(t) = \tfrac{1}{2}h_0(1+\cos^2 A)\cos\Psi(t), \tag{2}$$

$$h_\times(t) = h_0 \cos A \sin\Psi(t), \tag{3}$$

where

$$h_0 \equiv \frac{16G\epsilon I_{zz}\nu^2}{c^4 r}, \tag{4}$$

and where $\Psi(t)$ is the phase of the gravitational wave signal, A is the angle between the total angular momentum vector of the source and the direction from the star to the Earth (inclination angle), ν is the signal spin frequency, c and G are the light velocity and the gravity constant, respectively, and r is the distance from the source to the Earth. The ellipticity, ϵ, is defined as

$$\epsilon = \frac{I_{xx} - I_{yy}}{I_{zz}}. \tag{5}$$

where I_{xx}, I_{yy} and I_{zz} are the principal moment of inertia of the neutron star.

Antenna pattern. Antenna-pattern functions can be written as [11, 12]

$$F_+(t) = \sin\xi\{a(t)\cos 2\psi + b(t)\sin 2\psi\}, \tag{6}$$

$$F_\times(t) = \sin\xi\{b(t)\cos 2\psi - a(t)\sin 2\psi\}, \tag{7}$$

where ψ is a polarization angle; $a(t)$ and $b(t)$ are given by,

$$\begin{aligned} a(t) = {} & \tfrac{1}{16}\sin 2\gamma(3-\cos 2\lambda)(3-\cos 2\delta)\cos[2(\alpha-\phi_{\rm r}-\Omega_{\rm r}t)] \\ & -\tfrac{1}{4}\cos 2\gamma\sin\lambda(3-\cos 2\delta)\sin[2(\alpha-\phi_{\rm r}-\Omega_{\rm r}t)] \\ & +\tfrac{1}{4}\sin 2\gamma\sin 2\lambda\cos[\alpha-\phi_{\rm r}-\Omega_{\rm r}t] \\ & -\tfrac{1}{2}\cos 2\gamma\cos\lambda\sin 2\delta\sin[\alpha-\phi_{\rm r}-\Omega_{\rm r}t] + \tfrac{3}{4}\sin 2\gamma\cos^2\lambda\cos^2\delta, \end{aligned} \tag{8}$$

$$\begin{aligned} b(t) = {} & \cos 2\gamma\sin\lambda\sin\delta\cos[2(\alpha-\phi_{\rm r}-\Omega_{\rm r}t)] \\ & -\tfrac{1}{4}\sin 2\gamma(3-\cos 2\lambda)\sin\delta\sin[2(\alpha-\phi_{\rm r}-\Omega_{\rm r}t)] \\ & +\cos 2\gamma\cos\lambda\cos\delta\cos(\alpha-\phi_{\rm r}-\Omega_{\rm r}t) \\ & +\tfrac{1}{2}\sin 2\gamma\sin 2\lambda\cos\delta\sin(\alpha-\phi_{\rm r}-\Omega_{\rm r}t), \end{aligned} \tag{9}$$

where α and δ are the right ascension and the declination of the source, respectively, λ is the latitude of the detector's site, $\Omega_{\rm r}$ is the rotational angular velocity of the Earth, γ is the angle measured counterclockwise from the east to the bisector of the interferometer arms, ξ is the angle between the interferometer arms, and $\phi_{\rm r}$ is the deterministic phase of the Earth. Using equations (6) and (7), equation (1) can be written in the following form:

$$h(t) = S_+(t)\cos\Psi(t) + S_\times(t)\sin\Psi(t), \tag{10}$$

$$S_+(t) = \tfrac{1}{2}h_0\sin\xi(1+\cos^2 A)\{a(t)\cos 2\psi + b(t)\sin 2\psi\}, \tag{11}$$

$$S_\times(t) = h_0\sin\xi\cos A\{-a(t)\sin 2\psi + b(t)\cos 2\psi\}. \tag{12}$$

Values of known parameters used for the antenna pattern are shown in table 1. The location information of the pulsar is obtained from the Australia Telescope National Facility (ATNF) pulsar catalogue [13].

Phase evolution. The phase $\Psi(t)$ in equation (10) is assumed to be time dependent linearly for a short term. However, the phase will vary due to the influence of the spin down for the long term. The phase evolution of a pulsar can be modeled by using a Taylor expansion about a fixed fiducial time t_0 as follows:

$$\Psi(T) = \Psi_0 + 2\pi\left\{\nu_0(T-t_0) + \tfrac{1}{2}\dot{\nu}_0(T-t_0)^2 + \tfrac{1}{6}\ddot{\nu}_0(T-t_0)^3 + \cdots\right\}, \tag{13}$$

Table 1. Known parameters used for calculating an antenna pattern. α and δ are right ascension and declination of the source respectively. λ is latitude of the detector's site. Ω_r is rotational angular velocity of the Earth. γ is the angle measured counterclockwise from the east to the bisector of the interferometer arms. ξ is the angle between the interferometer arms.

α	08 h 35 m 20.61149 s
δ	−45 d 10 m 34.8751 s
λ	36.25° N
Ω_r	$2\pi/(0.9973 \times 24 \times 3600)$
γ	225°
ξ	90°

where Ψ_0 is the initial (epoch) spin phase, ν_0 and its time derivatives $\dot{\nu}_0$ are the pulsar spin frequency and spin-down coefficients at t_0 respectively, and T is the pulsar proper time. The values of $\nu_0, \dot{\nu}_0, \ldots$ are determined by radio observations. The phase evolution of a pulsar, equation (13), is Doppler shifted due to the relative velocity of the pulsar with respect to the solar system barycenter (SSB). Let the arrival time at the SSB to be t_b. Since the observed phase evolution with pulsar timing observations are also measured as Doppler shifted one, we set $t_b = T$. This is justified since PSR J0835-4510 is known to be an isolated pulsar, and the relative acceleration between the pulsar and SSB can be ignored within the observation period. A gravitational wave impinging on the interferometer will be modulated by Doppler shift, time delay and relativistic effects caused by the motions of the Earth and other bodies in the solar system. These effects can be written by the relation between observer coordinated time t into its arrival time at the SSB t_b as follows:

$$t_b = t + \delta t = t + \frac{\mathbf{r}\cdot\hat{\mathbf{n}}}{c} + \triangle_{E_\odot} + \triangle_{S_\odot}, \tag{14}$$

where the second term represents the Doppler shift due to the Earth's motion, $\mathbf{r}$ is the position of the detector with respect to the SSB, $\hat{\mathbf{n}}$ is the unit vector pointing to the pulsar in the SSB reference frame, the third term $\triangle_{E_\odot}$ is the Einstein delay which is generated by difference between terrestrial time frame and coordinate time frame in the SSB, and the last term $\triangle_{S_\odot}$ is the general relativistic Shapiro delay which is the time delay analog of the well-known bending of light at the limb of the sun [14]. We use the data in the HORIZONS system [15] for $\mathbf{r}$ in equation (14). The HORIZONS on-line solar system data and ephemeris computation service provide access to key solar system data and flexible production of highly accurate ephemerides for solar system objects. The HORIZONS data used for this search were down-sampled to 1/60 Hz.

In this search, the Shapiro delay (∼milliseconds) and the Einstein delay (∼micro seconds) were ignored because they are small compared with the Doppler term (∼hundreds seconds).

The most important variable is the frequency of the pulsar. Although the frequency of the pulsar changes with its spin-down frequency, it is mostly stable and follows the approximate model:

$$\nu(t) = \nu_0 + \dot{\nu}_0(t - t_0) + \ddot{\nu}_0(t - t_0)^2/2, \tag{15}$$

where $\dot{\nu}_0$ and $\ddot{\nu}_0$ are the first and second time derivatives of ν_0, respectively, and t_0 is a reference epoch. A *glitch* is a sudden frequency jump of magnitude $\Delta\nu/\nu$ from 10^{-9} to 10^{-6}, probably experienced in all ages of pulsars, but more frequently in younger pulsars. Once a glitch occurs, the evolution of the frequency does not follow the original curve line of equation (15). Then the latest information after the glitch has to be used for the signal template. The PSR J0835-4510 has been a particularly prolific source of glitches, having supplied us with 16

Table 2. The PSR J0835-4510 information after the 2006s glitch. ν_0 denotes a spin frequency. $\dot{\nu}_0$ and $\ddot{\nu}_0$ are a first derivative frequency and a second derivative frequency, respectively.

	Value	Uncertainty
ν_0 (Hz)	11.191 297 629 221 4275	0.000 000 001 577 1848
$\dot{\nu}_0$ (Hz s^{-1})	$-1.564\,376\,516\,769 \times 10^{-11}$	$6.594\,934\,679\,981 \times 10^{-16}$
$\ddot{\nu}_0$ (Hz s^{-2})	2.1035×10^{-21}	1.2704×10^{-22}

glitches since the glitch observation in 1969 [16]. We used the information of the PSR J0835-4510 after the last 2006s glitch before the observation of CLIO. Table 2 shows the information of the PSR J0835-4510 after the 2006s glitch[11], which is fitted using TEMPO [17, 18]. We use the frequency observed on MJD54083.00 (14 December 2006). The derivatives, $\dot{\nu}_0$ and $\ddot{\nu}_0$, are derived by fitting the data during MJD54109.801(9 January 2007) ∼MJD54175.602 (16 March 2007). We then obtain the frequency ν_0 at $t_0 =$ MJD54144. The frequency and its derivatives are summarized in table 2. In this search, we have to satisfy the accuracy of the frequency $\sim 5 \times 10^{-7}$ in order to suppress the SNR loss within 1%. The pulsar's frequency information satisfies these criteria. Therefore we can ignore the SNR loss due to the pulsar frequency uncertainty.

The frequency band ±0.003 (Hz) is adopted to derive the background distribution of the power at a frequency different from the target frequency.

3.2. Matched filtering

Time domain data from the detector, $x(t)$, can be considered as the sum of signal $h(t)$ plus noise $n(t)$,

$$x(t) = h(t) + n(t). \tag{16}$$

When we consider the narrow-banded signals like pulsar signals, the matched filtering is equivalent to compute the following quantity:

$$c = \int_0^{T_{\rm obs}} x(t)h(t)\,\mathrm{d}t, \tag{17}$$

where $T_{\rm obs}$ is the observation time. The phase function of signal is written as

$$\Psi(t) = 2\pi\nu_0(t - t_0) + \Psi'(t), \tag{18}$$

$$\Psi'(t) \equiv \Psi_0 + 2\pi\delta t + 2\pi\left\{\tfrac{1}{2}\dot{\nu}_0(t + \delta t - t_0)^2 + \tfrac{1}{6}\ddot{\nu}_0(t + \delta t - t_0)^3 + \cdots\right\}. \tag{19}$$

We can rewrite c as

$$c = 2\mathrm{Re}\int_0^{T_{\rm obs}} x'(t)\,\mathrm{e}^{2\pi\mathrm{i}\nu_0(t-t_0)}\,\mathrm{d}t, \tag{20}$$

$$x'(t) \equiv \frac{1}{2}(S_+ - \mathrm{i}S_\times)x(t)\,\mathrm{e}^{\mathrm{i}\Psi'(t)}. \tag{21}$$

This means that the matched filtering is equivalent to the computation of the Fourier transformation of the modulated data $x'(t)$.

[11] This value is obtained privately from the Australia Telescope National Facility (ATNF) young pulsar timing group.

The waveform has two unknown parameters, the inclination angle $A \in [0, \pi]$ and polarization angle $\psi \in [-\pi/4, \pi/4]$. In this analysis, since the number of unknown parameters is not very large, we search for these two parameters which maximize c as a straightforward analysis strategy. In order to keep the loss of SNR as low as 2%, we consider 6 values, $(3/8\pi, 7/16\pi, 31/64\pi, 33/64\pi, 9/16\pi, 5/8\pi)$, for the inclination A, and 17 values spaced equally in $[-\pi/4, \pi/4]$ for ψ.

3.3. Data conditioning

In this subsection, we explain the method of the data compression and the removal of the low-quality data. Some of these methods are based on [6].

In order to reduce the computation time of the analysis, the down-sampling is done with the complex heterodyne technique (CHT) [6]. We shift arbitrary frequency components of the signal to DC (0 Hz), and we reduce the data by down-sampling. The CLIO data are sampled at 65 536 Hz frequency. We introduce a two stage down-sampling method. In the first stage, a simple moving boxcar average of 512 data points, which is called boxcar filter [6], is used as an anti-aliasing filter. These low-passed data are re-sampled to 256 Hz. In the second stage, we compress re-sampled data from 256 Hz to 1 Hz by using an IIR digital filter [19]. Before the second stage, the data are transferred from the voltage data to the displacement data.

The observational data from the interferometer do not obey the simple stationary, Gaussian process. They contain transient noise, such as short spike noise, due to instability of the interferometer. The data which contain such short spike noise are removed, and the gap of the data is padded with zero. The data for 128 s, before the lock of the interferometer is lost and after the lock is recovered, are removed from the analysis, because such data may not be calibrated properly.

The average noise level of the data varies due to environmental disturbances, such as fluctuation of temperature, atmosphere pressure, seismic noise level and so on. These degrade the SNR of signals. In order to reduce the influence of such low-quality data, we introduce weighting function to the data so that the data with lower noise level make the highest contribution to the overall SNR. In the weighting function, the correction corresponding to the amplitude modulation of the signal is also introduced. This method is based on [6].

After applying these data quality filters, the length of the data was reduced from 86 h to 57 h.

4. Results

After data conditioning, we compute equation (21) by using FFT. The powers in a frequency range of $-0.003 < \nu < 0.003$ (Hz) are computed.

In figure 2, a histogram of the power, P, computed with the parameters of a template, $A = 31/64\pi$ and $\psi = 1/4\pi$, is shown. This template produces the largest power. The largest power at the zero frequency, where the pulsar signal should exist if it would be produced, is $P = 0.3P_0$, where P_0 is the mean of the power and given as $P_0 = 4.79 \times 10^{-31}$ ($\mathrm{m}^2\ \mathrm{Hz}^{-1}$). The largest power at the zero frequency is indicated by an arrow in figure 2. This value is completely consistent with the assumption that it is produced by noise. We conclude that we do not have any significant signal which could be identified as a real gravitational wave signal.

In the case of stationary, Gaussian noise, the distribution of the power is given by [6]

$$f(P) = \frac{N \times \omega_{\mathrm{bin}}}{P_0}\, \mathrm{e}^{-\frac{P}{P_0}}, \tag{22}$$

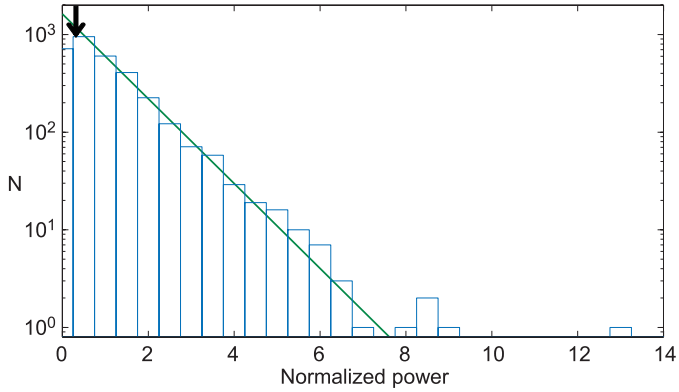

Figure 2. A histogram of the power with parameters, $A = 31/64\pi$ and $\psi = 1/4\pi$. The solid line is the theoretical line, equation (22). The arrow indicates the largest power at the targeted frequency (0 Hz).

where $\omega_{\rm bin} = 4.8 \times 10^{-31}$ (m^2 Hz^{-1}) is the size of bins of the power used to plot the histogram, $N = 3245$ is the number of frequency bins, and P_0 is the mean of the power given as $P_0 = 4.79 \times 10^{-31}$ (m^2 Hz^{-1}). With these parameters, we plot equation (22) in figure 2 with a solid line. We find that the distribution of the power agrees with equation (22) excellently except at the tail, $P = 13.18P_0$. Although the frequency which produces $P = 13.18P_0$ is different from 0 (Hz), we set the threshold on the power at $P_{\rm T} = 13.18P_0$ in order to derive a conservative upper limit[12]. The probability of finding power less than the threshold P_T is

$$\mathcal{P}_0 = 1 - \exp\left(-\frac{P_T}{P_0}\right). \tag{23}$$

The probability of detecting a false alarm originating from the noise in any of N independent frequency points can be found by using the Poisson distribution with a mean $\mu = N\mathcal{P}_0$. The false alarm probability becomes

$$\mathcal{P}_1 = \mu\, \mathrm{e}^{-\mu}. \tag{24}$$

We find that the false alarm probability corresponding to the above threshold is 0.6%.

The upper limit on the gravitational wave amplitude is given by

$$h_{0(\rm UL)} = \frac{\sqrt{2P_{\rm T}[\mathrm{m}^2\ \mathrm{Hz}^{-1}] \triangle \nu}}{L}, \tag{25}$$

where $\triangle\nu$ is a frequency resolution and L is an arm length of the interferometer. We substitute $\triangle\nu = 1.8491 \times 10^{-6}$ (Hz) and $L = 100$ (m) to equation (25), and obtain an upper limit on the gravitational wave amplitude of 4.8×10^{-20}. As a systematic error, we take into account the calibration error. We assume that the calibration error is at most 10%. This produces a systematic error to the upper limit, $\pm 4.8 \times 10^{-21}$. We take the larger value of the error, and obtain a conservative upper limit, $h_{0(\rm UL)} = 5.3 \times 10^{-20}$. We can interpret this value as the upper limit on the ellipticity ϵ of the neutron star, which becomes $\epsilon = 29$.

[12] We may obtain a better upper limit by using the Bayesian method proposed in [21]. However, we did not adopt that approach in this paper. We leave this point as a future work.

5. Summary

A search for gravitational waves from PSR J0835-4510 (Vela pulsar) was performed in the CLIO data taken during 12–18 February 2007. Searches for sources with spin frequencies less than 25 Hz had never been attempted before, since previous gravitational wave detectors did not have good sensitivity in this band. The CLIO data had good sensitivity in the low-frequency range, and this was the first attempt to analyze PSR J0835-4510 by using interferometer data.

We used the matched filtering method to search for the pulsar signal. We also used the complex heterodyne technique to compress the data without losing the information of the signal. We used the parameters of the PSR J0835-4510 after the latest glitch on August 2006. The spin frequency information obtained in December 2006 and the spin down information obtained from January to March 2007 were used. The parameters which produce the largest power of the signal are searched in the parameter space of two unknown parameters, the polarization angle and the inclination angle. The search was done in the frequency range $\nu_0 - 0.003 < \nu < \nu_0 + 0.003$ (Hz) around the target signal frequency. The total length of data analyzed was 57 h. We did not find any significant signals which could be identified as real gravitational wave signals. We obtained an upper limit of $h_{0(\mathrm{UL})} = 5.3 \times 10^{-20}$ at 99.4% confidence level. This value corresponds to the upper limit on the ellipticity of the neutron star, $\epsilon = 29$.

Although the upper limit we obtained is not very stringent, this result shows that the analysis in such a low-frequency region can be done with an interferometer detector in very quiet environment, such as in the Kamioka mine. This is good news for future detectors, especially for LCGT [9].

Acknowledgments

We thank the Australia Telescope National Facility (ATNF) young pulsar timing project for providing us with the information about PSR J0835-4510. We would also like to thank John Mirror and Hiroaki Yamamoto for carefully reading the manuscript. This work was supported in part by the Grant-in-Aid for Scientific Research on Priority Areas (415) of the Ministry of Education, Culture, Sports, Science and Technology of Japan, and in part by JSPS Grant-in-Aid for Scientific Research nos 13048101 and 18204021.

References

[1] Abbott B *et al* 2004 *Nucl. Instrum. Methods* A **517** 154
[2] Willke B *et al* 2004 *Class. Quantum Grav.* **21** S417
Lück H *et al* 2006 *Class. Quantum Grav.* **23** S71
[3] Takahashi R (for the TAMA Collaboration) 2004 *Class. Quantum Grav.* **21** S403
Ando M *et al* (the TAMA Collaboration) 2001 *Phys. Rev. Lett.* **86** 3950
[4] Acernese F *et al* 2004 *Class. Quantum Grav.* **21** S385
Acernese F *et al* 2006 *Class. Quantum Grav.* **23** S63
[5] Hobbs G *et al* 2005 *Mon. Not. R. Astron. Soc.* **360** 974
Page D *et al* 1996 *MPE Rep.* **263** 173
Gupta Y *et al* 1995 *Astrophys. J.* **451** 717
Taylor J H *et al* 1993 *Astrophys. J. Supp.* **88** 529
[6] Niebauer T M *et al* 1993 *Phys. Rev.* D **47** 3106
Soida K *et al* 2003 *Class. Quantum Grav.* **20** S645
[7] Takemoto S *et al* 2006 *J. Geodyn.* **41** 23
[8] Miyoki S *et al* (CLIO Collaboration) 2006 *Class. Quantum Grav.* **23** S231
Yamamoto K *et al* (CLIO Collaboration) 2008 *J. Phys.: Conf. Ser.* **122** 012002

[9] Kuroda K (LCGT Collaboration) 2006 *Prog. Theor. Phys. Suppl.* **163** 54
[10] Telada S *et al* 2000 *Proc. 2nd TAMA Int. Workshop on Gravitational Wave Detection, Frontiers Science Series No 32* (Tokyo: Universal Acadamy Press)
[11] Jaranowski P, Królnk A and Schutz B F 1998 *Phys. Rev.* D **58** 063001
[12] Bonazzola S and Gourgoulhon E 1996 *Astron. Astrophys.* **312** 675
[13] http://www.atnf.csiro.au/research/pulsar/psrcat/
[14] Shapiro I I 1964 *Phys. Rev. Lett.* **13** 798
[15] http://ssd.jpl.nasa.gov/
[16] Radhakrishnan V and Manchester R N 1969 *Nature* **222** 228
[17] Hobbs G B, Edwards R T and Manchester R M 2006 *Mon. Not. R. Astron. Soc.* **372** 1549
[18] Hobbs G B, Edwards R T and Manchester R M 2006 *Mon. Not. R. Astron. Soc.* **369** 655
[19] Proakis J G and Manolakis D G 2007 *Digital Signal Processing* (Englewood Cliffs, NJ: Pearson/Prentice-Hall)
[20] Hobbs G, Lorimer D R, Lyne A G and Kramer M 2005 *Mon. Not. R. Astron. Soc.* **360** 974
[21] Dupuis R J and Woan G 2005 *Phys. Rev.* D **72** 102002